ICAS 2021 SHANG HAI
International Council of the Aeronautical Sciences
32nd Congress of the International Council of the Aeronautical Sciences
September 6-10, 2021
Pudong Shangri-La, Shanghai, China

Subsonic wind tunnel small riblets drag reduction experiment on C919 fuselage model

Hongwei wang[1], Zhan Huang[1], Minglei Yuan[1], Xiaohui Li[1], Miao Zhang[2]

[1]China Academy of Aerospace Aerodynamics, Beijing, China
[2]Shanghai Aircraft Design and Research Institute, Shanghai, China

Abstract

Small riblets grooves is one of the important means of turbulence drag reduction of aircraft. When the civil aircraft flies in the cruise state, the flow in most parts of the body is in a turbulent state, so it's significant to study the drag reduction of small riblets in the turbulent boundary layer. A type of small riblet film suitable for subsonic wind tunnel flow field (Ma0.6-Ma0.82) was designed for the C919 fuselage model and compared with the smooth film. Also, the balance force test and PIV flow field measurement test were carried out respectively. The balance force test was used to compare the force of the body model with small riblets film or smooth film attached on Mach 0.75 and Mach 0.785, and the total drag coefficient was reduced by about 1%-2%. The PIV test measured the longitudinal symmetry plane velocity field on the upper part of the fuselage with different film attached, and the test Mach number were 0.75, 0.785 and 0.82. The PIV result showed that the flow velocity above the small riblets film was slightly higher, and the turbulence intensity and turbulent kinetic energy were all reduced. These test results illustrated that the small riblets could effectively reduce the turbulent frictional resistance of the fuselage model.

Keywords: turbulence drag reduction, small riblets, subsonic, PIV

1. General Introduction

For general civil aviation aircraft, the skin friction accounts for about 50% of the total drag, the drag reduction is not only directly related to the performance of civil aviation aircraft, but also indirectly affect the flight cost and environment. Study on drag reduction can be traced back to the 1930s, but until the mid-1960s, research work focused on the reduction of the surface roughness, which implicit assumption is that the smooth surface has least resistance. After that, scientists through different flow experiments showed that: the smooth surface is not the best way is to drag reduction as classical Darcy experiment described. After the 1970s NASA Langley Research Center found the riblet grooves along the flow direction can effectively reduce skin friction[1], which broke the way of thinking that smoother surface had less drag, the drag reduction by riblet grooves became popular subject in turbulent drag reduction. After lots of research work[2][3][4], many experts and scholars' research agree that the riblet grooves along the flow direction with $h+\leq 25$ and $s+\leq 30$ have drag reduction effect. At present, the research abroad has entered the engineering practical stage. The United States, Europe, Russia and Japan have all launched the research on the application of small riblets surface drag reduction[5].

Large civil aviation aircraft usually has large fuselage length, such as C919 fuselage length is more than 38 meters, so that most of the fuselage area is in turbulent state in cruise state. Then the effect of turbulent drag reduction by using small riblets flow control means on the fuselage surface will be more obvious.

In this paper, a set of experimental verification methods for suppressing the turbulent skin friciton of C919 fuselage model with small riblets are developed based on the balance force test and PIV flow field measurement test.

2. C919 Fuselage Model and Small Riblets Film

2.1 C919 Fuselage Model

The C919 fuselage model without wings and tail was used as the test model in a 1.2m transonic wind tunnel. The total length of the model was 1300mm, and the measurement center of the balance was designed at 520mm of the leading edge. In the flow direction, the model is divided into four sections, which are the nose section, the front section, the middle section and the tail section. The balance is connected with the middle section, and the tail section of the balance is connected with the angle of attack mechanism of the wind tunnel through a strut. In order to maximize the drag reduction effect of the riblets film, it is planned to attach a large area of riblets film on the surface of the wing model as far as possible. However, due to the irregular surface of the fuselage head and tail, the actual adhesion length of rib film is 600mm, which is from 220mm to 820mm at the leading edge of the fuselage, and a forced transition trips is set at the front of the riblets film.

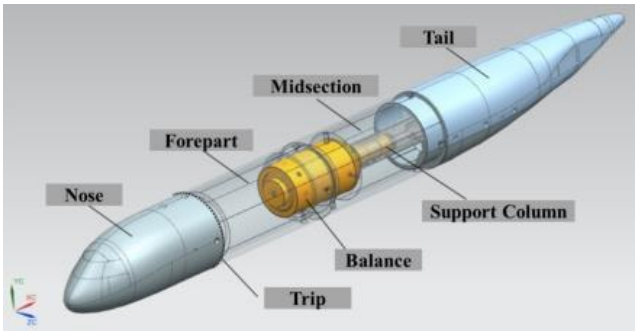

Figure 1 – Sketch of C919 fuselage model

2.2 General Procedures for Submission

The low speed flow field does not consider the compressibility and heat exchange, and the friction velocity can be obtained directly by calculating the friction coefficient of the specific position of the model. However, the structure of the high speed boundary layer is the same as that of the low velocity boundary layer, so the friction coefficient of the compressible flow can be calculated by the formula of the friction coefficient of the incompressible flow. The compressibility (by Mach Number acting) and heat exchange (by T_w/T_e acting) only affect the temperature in the boundary layer and the temperature related quantities (density, viscosity). Therefore, if the temperature in the low-speed boundary layer and the quantity related to the temperature are corrected, and a reference temperature is taken to replace the original temperature, then the friction coefficient formula of the low-speed boundary layer can be used to calculate the friction coefficient of the high-speed boundary layer. Based on the theoretical calculation and experimental results, the reference temperature T^* can be approximately determined by Eckert (1995) formula

$$T^*=T_\infty+0.5(T_w-T_\infty)+0.22(T_w-T_\infty) \tag{1}$$

At the same Reynolds number, it can be obtained that

$$\frac{C_{f\text{-}Compressible}}{C_{f\text{-}Incompressible}}=\left(\frac{T^*}{T_\infty}\right)^{\frac{\omega\text{-}4}{5}}=\left(\frac{T^*}{T_\infty}\right)^{-0.648} \tag{2}$$

According to the formula and wind tunnel flow conditions, the leading edge, center and end position of the riblets parameter are selected as the reference length, and the normalized friction scale calculated are shown in Table 1. The friction scale on Mach number 0.785 and 520mm reference length is selected to complete the design and processing of the riblets film.

Table 1 – The normalized parameter of riblets

Mach	λ*(220mm)/μm	λ*(520mm)/μm	λ*(820mm)/μm
0.7	1.8618	2.0291	2.1236
0.785	1.7417	1.8982	1.9867
0.8	1.7242	1.8791	1.9667

0.82	1.7023	1.8553	1.9417

3. Force comparison test

The force test of the fuselage model small riblets film drag reduction balance is carried out by using six component strain balance, and the balance code is n636fa whose minimum resistance resolution is 70g. By comparison, the same area of small riblets would be replaced by smooth film.

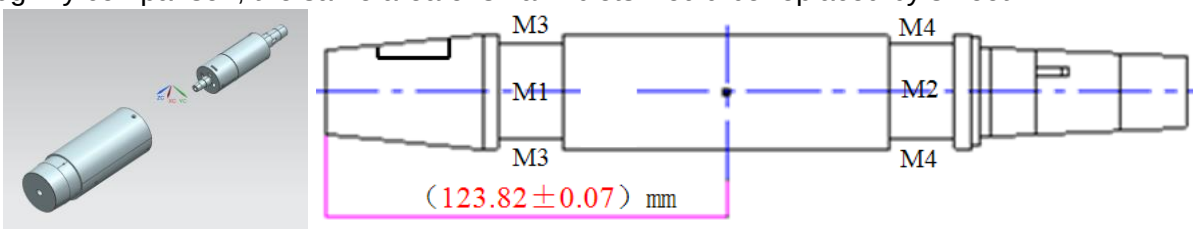

Figure 2 – Sketch of Blance

Table 2 – The force comparison test condition

Mach	Riblets film	Smooth film
0.75	Riblet1/ Riblet2/ Riblet3	Smooth1/ Smooth2/ Smooth3
0.785	Riblet1/ Riblet2/ Riblet3	Smooth1/ Smooth2/ Smooth3

Two Mach numbers (Ma=0.75 and Ma=0.785) were measured in the force comparison test of thin film drag reduction balance with small ribs of fuselage model. Figure 3 shows the comparison of lift and drag coefficients between riblets film and smooth film at Ma=0.75, Figure 4 shows the comparison of lift and drag coefficients between riblets film and smooth film at Ma=0.785.

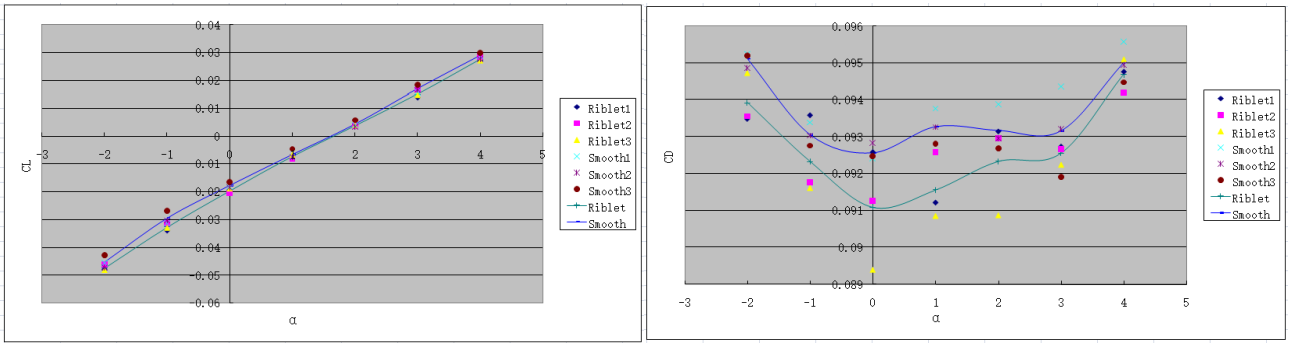

Figure 3 – CL/CD of the model with Riblets film or Smooth film(Ma=0.75)

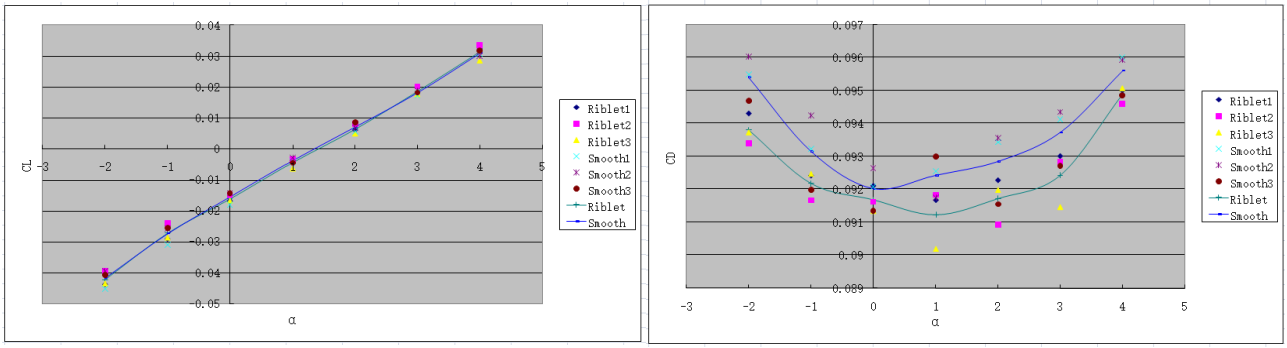

Figure 4 – CL/CD of the model with Riblets film or Smooth film(Ma=0.785)

Table 3 – The drag reduction rate of riblet film relative to smooth film

α	-2	-1	0	1	2	3	4
Ma=0.75	1.2598	0.7978	1.6395	1.8896	0.9242	0.6663	0.3344
Ma=0.785	1.7019	1.0521	0.3598	1.3042	1.2209	1.4027	0.7481

It can be seen from the result that under the condition of Ma=0.75, the lift of fuselage model changes little, and the drag coefficient distribution with angle of attack is similar to that of smooth film but significantly decreased, which reaches a very low value near zero angle of attack and increases at positive and negative angles of attack. Under the condition of Ma=0.82, the lift of fuselage model changes little too, and the drag coefficient distribution with angle of attack is similar to that of smooth

film but significantly decreased too, which reaches a very low value near zero angle of attack and increases at positive and negative angles of attack. Table 3 shows the drag reduction rate of riblet film relative to smooth film, which effectively verifies the drag reduction effect of small riblets film.

4. PIV Flow Field Test

Table 4 – The PIV flow field test condition

Ma	0.75	0.785	0.82
Smooth film	√	√	√
Riblets film	√	√	√

The PIV experimental layout of fuselage small riblets film drag reduction verification is shown in Figure 5. The optical damping platform is set up above the perforated plate of the experimental section and the laser and the light guide arm with a length of 0.6m is fixed on the platform. The Nd:YAG Laser makes two 300mJ laser pulses at 10Hz. The CCD camera with 2048×2048 pixels is placed in the side interlayer, and the flow field photos are taken through the side window.

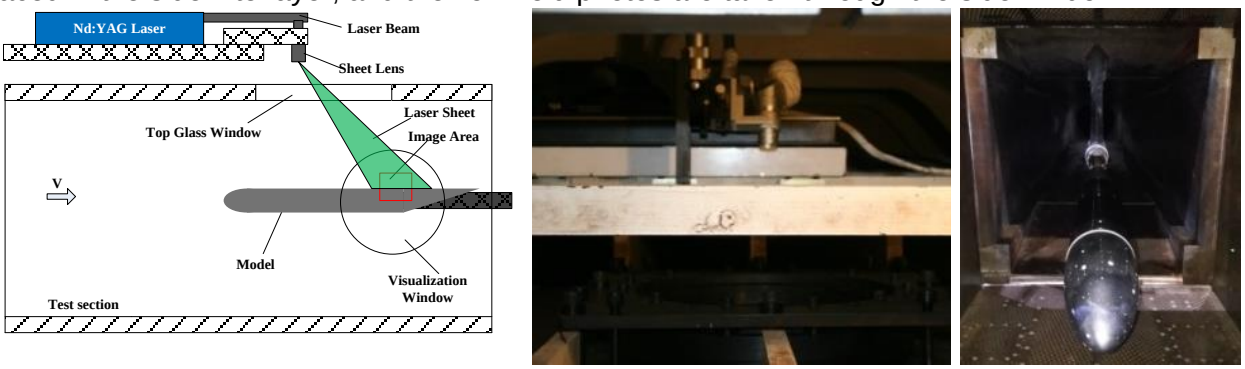

Figure 5 – The test set of PIV experimental

Before the DPIV experiment, the ruler is first placed in the experimental area and photographed with a CCD camera to determine the size of the actual measurement area and the proportional relationship between the CCD camera pixel and the size of the calibration plate. According to the total temperature of the flow and the Mach number of the experimental area, the approximate velocity of the experimental area can be determined. According to the actual space represented by the CCD camera pixels and the proposed number of displacement pixels, the laser pulse exposure spacing can be determined. In the DPIV experiment, the wind tunnel should be run first, and then the particle generator should be turned on for CCD camera shooting. In order to eliminate the influence of stray light, a narrow band color filter (532± 5nm) is installed before the CCD camera. The focal length of CCD camera is 200 mm and the thickness of laser sheet is 1 mm.

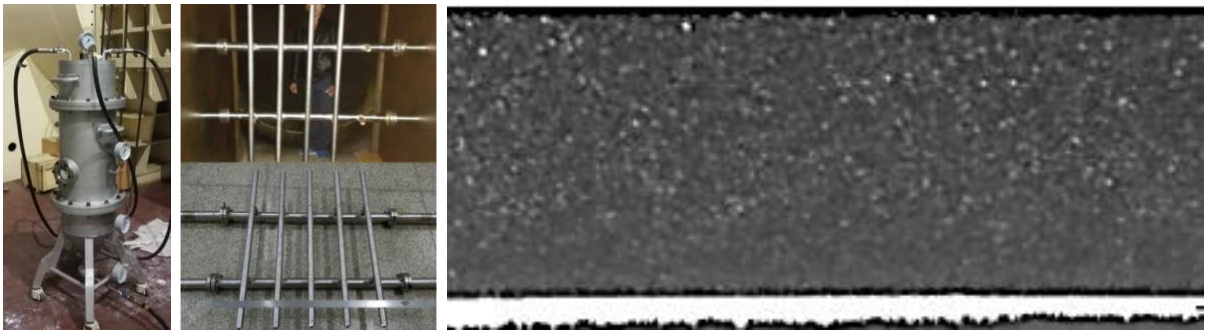

Figure 6 – The particle generator and paticle image example

In order to calculate PIV better, it is necessary to unify the model boundary in the particle image to the same position. Therefore, the image correction methods were introduced to recognize the model boundary in the image, and batch translation processing was used on the image to constrain the model boundary in each image with a unified position.

Comparing the PIV results of smooth film and small riblets film, the drag reduction effect of small rib film will be analyzed by investigating the average velocity distribution, turbulence intensity $I(j, k)$ and turbulent kinetic energy $\kappa_i(j, k)$ of boundary layer flow.

$$I(j,k)=\frac{\sqrt{\frac{\sum_{i=1}^{n}\left(u_i'(j,k)\right)^2}{n}}}{\overline{u(j,k)}},\quad \kappa(j,k)=\left(u_i'(j,k)\right)^2+\left(v_i'(j,k)\right)^2 \tag{3}$$

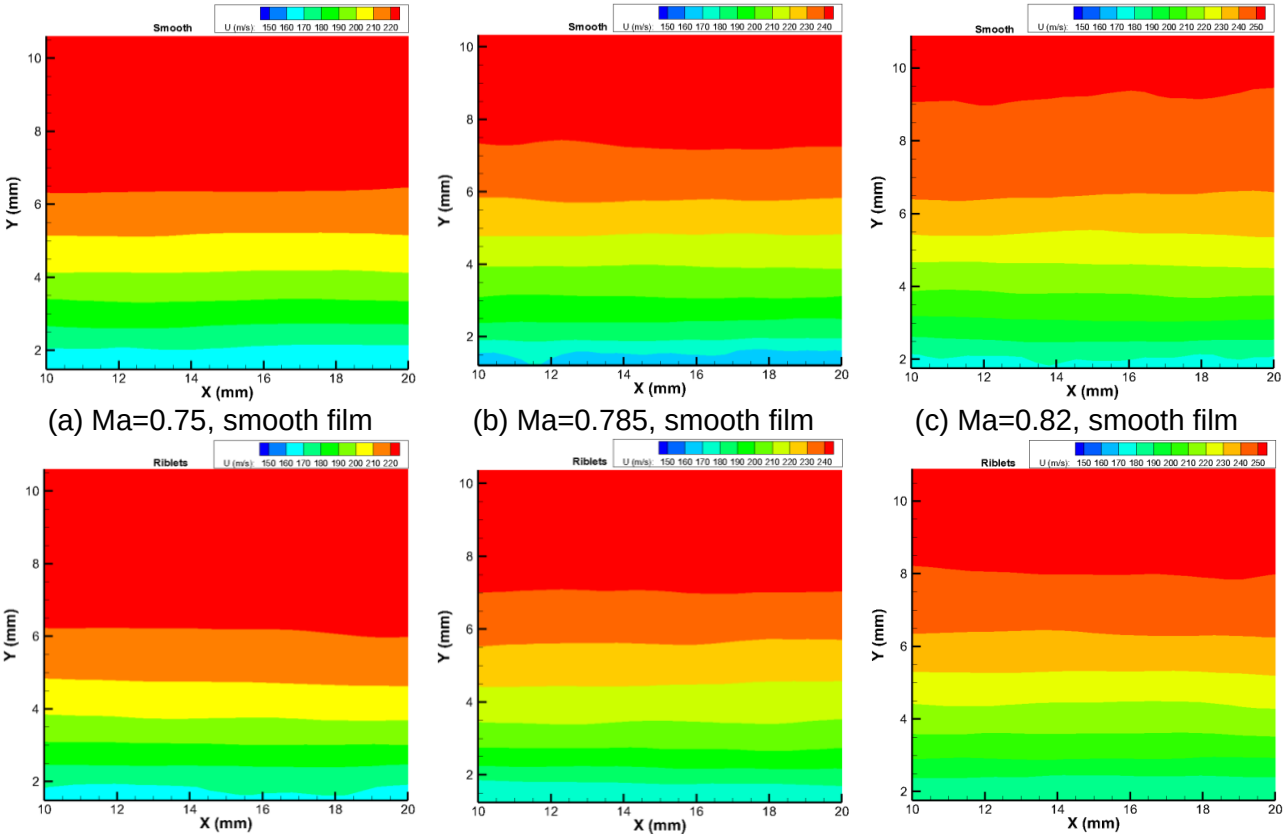

(a) Ma=0.75, smooth film (b) Ma=0.785, smooth film (c) Ma=0.82, smooth film

(d) Ma=0.75, riblets film (e) Ma=0.785, riblets film (f) Ma=0.82, riblets film

Figure 7 –The average velocity distribution of test area with Riblets film or Smooth film

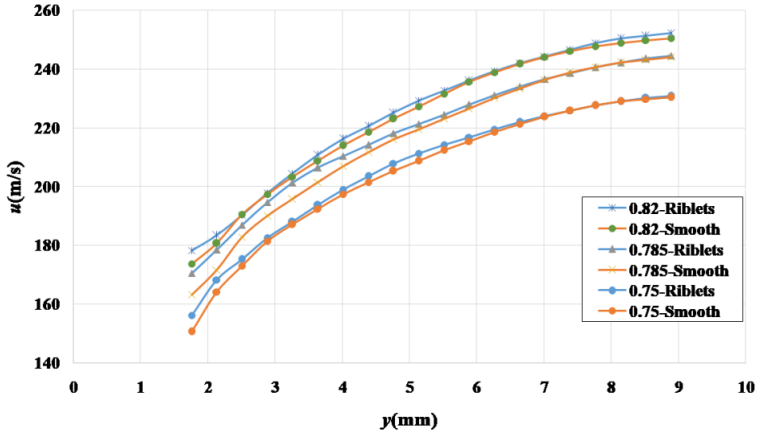

Figure 8 –The average velocity curve of Riblets film and Smooth film

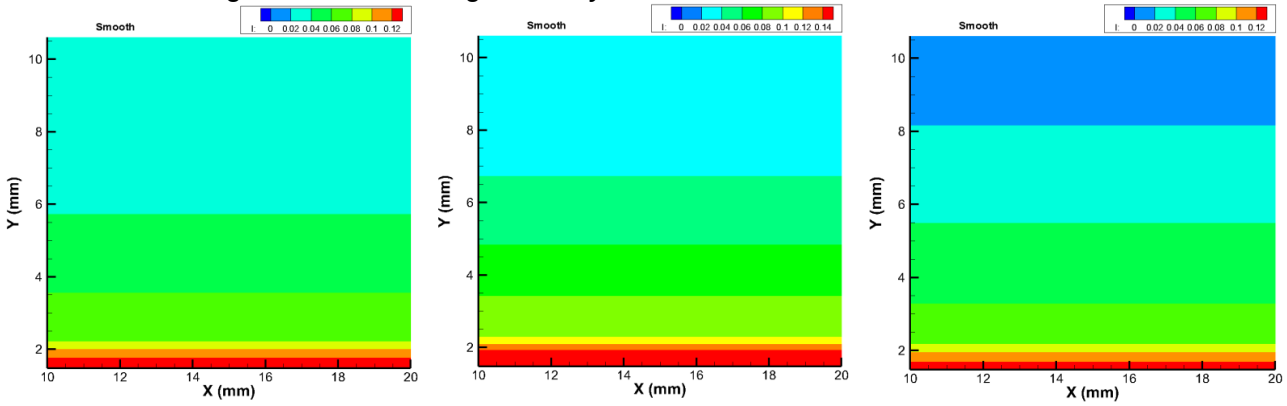

(a) Ma=0.75, smooth film (b) Ma=0.785, smooth film (c) Ma=0.82, smooth film

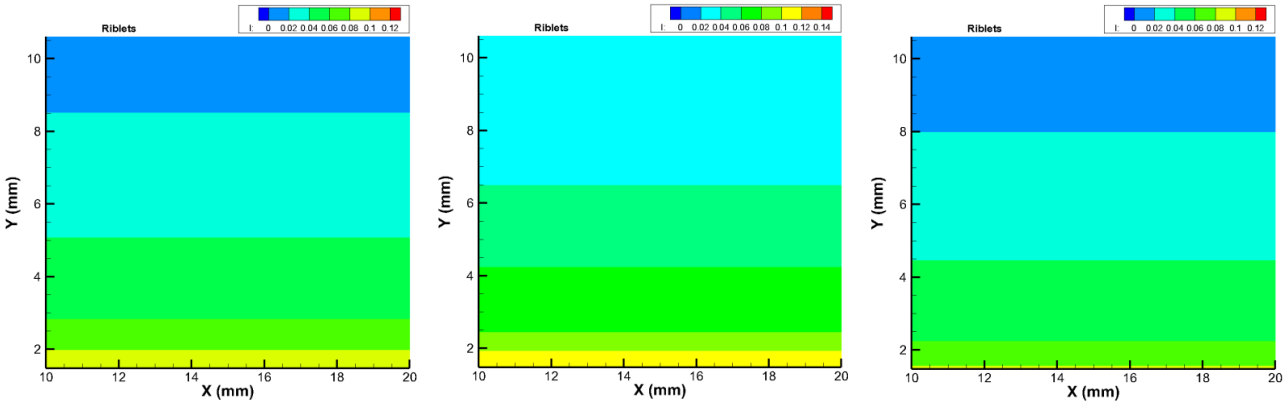

(d) Ma=0.75, riblets film (e) Ma=0.785, riblets film (f) Ma=0.82, riblets film

Figure 9 –The turbulence intensity of Riblets film and Smooth film

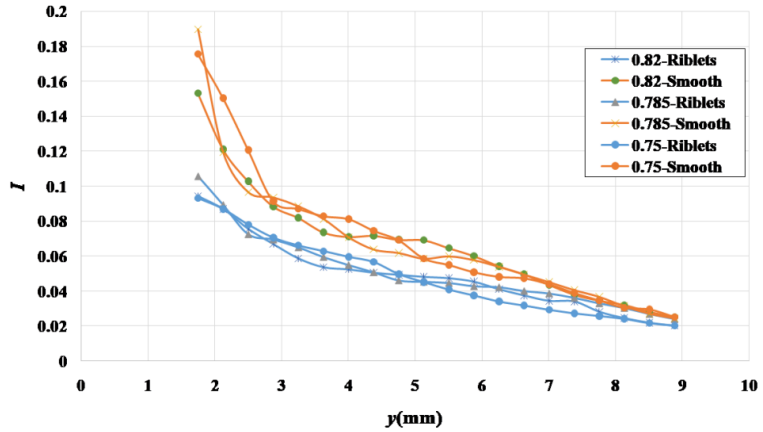

Figure 10 –The turbulence intensity curve of Riblets film and Smooth film

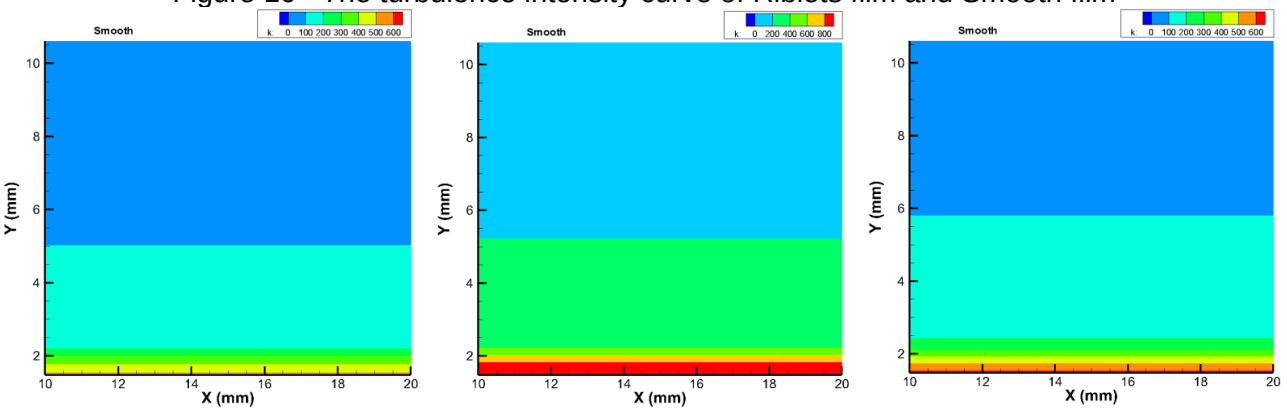

(a) Ma=0.75, smooth film (b) Ma=0.785, smooth film (c) Ma=0.82, smooth film

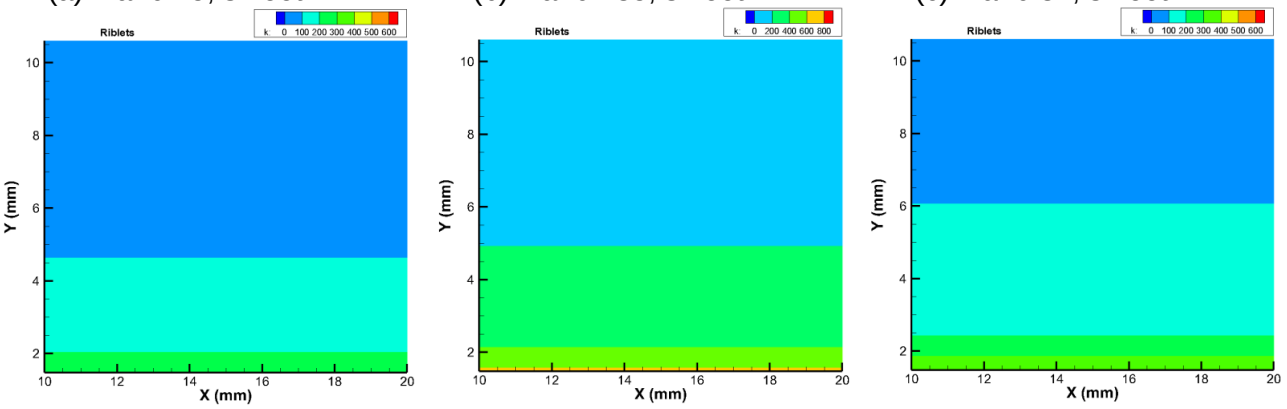

(d) Ma=0.75, riblets film (e) Ma=0.785, riblets film (f) Ma=0.82, riblets film

Figure 11 –The turbulence kinetic energy of Riblets film and Smooth film

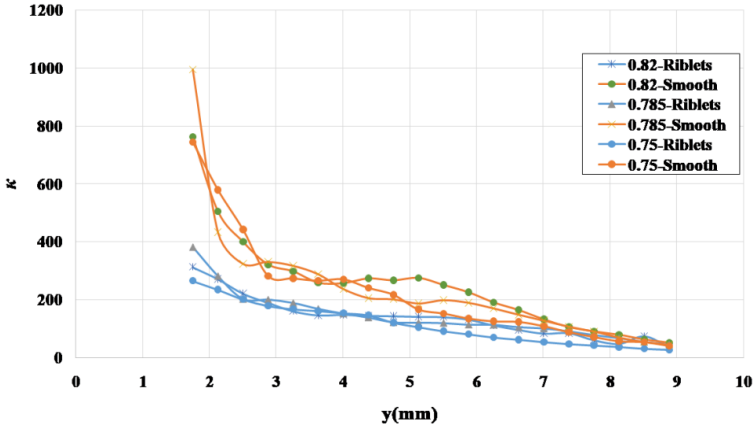

Figure 12 –The turbulence kinetic energy curve of Riblets film and Smooth film

It can be seen that at the flow condition of Ma=0.75, Ma=0.785 and Ma=0.82, the main flow velocity above the small riblets film and smooth film is more than 230m/s, 245m/s and 250m/s. There is no significant difference in the average velocity of the flow field above the smooth film and the small riblets film near the mainstream. However, the average velocity of the flow field in the boundary layer along the wall increases slightly when the small riblets film is used.From the results of stream-wise turbulence intensity distribution result, it can be seen that at the flow condition of Ma=0.75, Ma=0.785 and Ma=0.82, the stream-wise turbulence intensity distribution above the small riblets film and smooth film is basically similar with a tending of increasing when close to the bottom. However, most of the stream-wise turbulence intensity above the small riblets film is below 10%, The turbulence intensity of the flow field above the smooth film reaches 15% - 20%.From the results of stream-wise turbulent kinetic energy distribution result, it can be seen that at the flow condition of Ma=0.75, Ma=0.785 and Ma=0.82, the turbulent kinetic energy above the small riblets film and smooth film is basically similar. However most of the equivalent turbulent kinetic energy above the small riblets film is below 400 m^2/s^2, The maximum turbulent kinetic energy of the flow field above the smooth film is 700-1000 m^2/s^2.The PIV results show that, after using small riblets film, the average velocity of flow direction in the boundary layer along the model wall increases slightly, and the turbulence intensity and turbulent kinetic energy decrease obviously. It can be proved that the existence of the small riblets film inhibits the turbulence intensity and has a beneficial effect on reducing the turbulent skin friction.

5. Conclusion

The balance force test and PIV flow field measurement test were carried out on the C919 fuselage model with riblets film or smooth film. The balance force test result showed that the total drag coefficient was reduced by about 1%-2%. The PIV test result showed that the flow velocity above the small riblets film was slightly higher, and the turbulence intensity and turbulent kinetic energy were all reduced. These test results illustrated that the small riblets could effectively reduce the turbulent frictional resistance of the fuselage model.

6. Copyright Statement

References

[1] Walsh M J. Turbulent boundary layer drag reduction using riblets [R]. American: AIAA, 1982.

[2] J M Caram, A Ahmedt. Devel. of the Wake of an Airfoil with Riblets[J]. AIAA Journal, 30(2), 1992.

[3] Wang J J, Lan S L. Effect of the riblets surface on the boundary layer development[J]. Chinese Journal of Aeronautics, 9(4), pp 257-260, 1996.

[4] Christoph P P. What is a shark doing in this pump [J]. World Pumps, 423, pp 15 - 16, 2001.

[5] Wang H W, Huang ZH. Global Skin Friction Measurement Technique Based on Fluorescent Oil Film Application in the Measurement of Riblets Drag Reduction[C], ISFV-18, Zurich, Switzerland, 2018.